

Detection of the diffuse supernova neutrino background with JUNO

Jie Cheng^{a,*} on behalf of the JUNO Collaboration

(a complete list of authors can be found at the end of the proceedings)

^a*Institute of High Energy Physics, Chinese Academy of Sciences,
Beijing, China*

E-mail: chengjie@ihep.ac.cn

As an underground multi-purpose neutrino detector with 20 kton liquid scintillator, Jiangmen Underground Neutrino Observatory (JUNO) is competitive with and complementary to the water-Cherenkov detectors on the search for the diffuse supernova neutrino background (DSNB). Typical supernova models predict 2-4 events per year within the optimal observation window in the JUNO detector. The dominant background is from the neutral-current (NC) interaction of atmospheric neutrinos with ^{12}C nuclei, which surpasses the DSNB by more than one order of magnitude. We evaluated the systematic uncertainty of NC background from the spread of a variety of data-driven models and further developed a method to determine NC background within 15% with *in situ* measurements after ten years of running. Besides, the NC-like backgrounds can be effectively suppressed by the intrinsic pulse-shape discrimination (PSD) capabilities of liquid scintillators. In this talk, I will present in detail the improvements on NC background uncertainty evaluation, PSD discriminator development, and finally, the potential of DSNB sensitivity in JUNO.

*37th International Cosmic Ray Conference (ICRC 2021)
July 12th – 23rd, 2021
Online – Berlin, Germany*

*Presenter

1. Introduction

The integrated flux of neutrinos from all past core-collapse supernovae in the visible universe form the diffuse supernova neutrino background (DSNB), which carries valuable information on the cosmic star-formation rate, the average core-collapse neutrino spectrum, and the rate of failed SNe. The existing and future large water-Cherenkov (wCh) and liquid-scintillator (LS) detectors have good potential to observe the DSNB via the inverse-beta-decay (IBD) reaction, $\bar{\nu}_e + p \rightarrow e^+ + n$, which consists of a prompt signal of positron and a delayed signal of neutron capture. The event rate of the DSNB is very rare. So far, no appreciable IBD signal events of the DSNB $\bar{\nu}_e$ have been found in wCh and LS detectors.

Comparing to the wCh detectors, the LS detectors have lower energy thresholds, higher energy resolution, and more than 99% neutron tagging capability. The dominant background is from the neutral-current (NC) interactions of atmospheric neutrinos with the carbon nuclei in LS. JUNO [1, 2] consists of a 20 kt liquid scintillator (LS) detector. Depending on the DSNB model, we expect about 2–4 IBD events per year in the energy range above the reactor $\bar{\nu}_e$ signal. Given the excellent light yield, the delayed signal from neutron capture on hydrogen in the LS offers a efficient tag for background reduction, while pulse-shape discrimination helps to suppress the background from atmospheric neutrino NC interactions. Hence, JUNO is competitive with and complementary to the wCh detectors like SuperK-Gd.

2. DSNB signal prediction

The DSNB signal spectrum in detector in terms of the measured energy (E_{prompt}) is given by:

$$\frac{dS(E_{\text{prompt}})}{dE_{\text{prompt}}} = N_p \times \sigma(E_\nu) \times J(E_\nu) \times \frac{d\phi}{dE}(E_\nu), \quad (1)$$

where, N_p is the number of protons of JUNO LS. $\sigma(E_\nu)$ is the energy dependent IBD cross section [3]. $J(E_\nu)$ is the Jacobian factor, which is used to convert $dS(E_\nu)/dE_\nu$ to $dS(E_{\text{prompt}})/dE_{\text{prompt}}$. The last term is the DSNB flux, which can be obtained by

$$\frac{d\phi}{dE_\nu} = \int_0^5 R_{\text{SN}}(z) \frac{dN(E'_\nu)}{dE'_\nu} (1+z) \left| \frac{cdt}{dz} \right| dz, \quad (2)$$

where c is the speed of light, $|dt/dz|^{-1} = H_0(1+z)[\Omega_\Lambda + \Omega_m(1+z)^3]^{-\frac{1}{2}}$ includes the Hubble constant ($H_0 = 70 \text{ km} \times \text{s}^{-1} \times \text{Mpc}^{-1}$) and the ratios of the energy density of matter and the cosmological constant ($\Omega_\Lambda = 0.7$ and $\Omega_m = 0.3$). Due to the red shift effect, a neutrino received at the energy E_ν was emitted at a higher energy $E'_\nu = E_\nu(1+z)$. Hence, the factor $(1+z)$ on the spectrum accounts for the compression of the energy scale. dN/dE_ν is the average SN neutrino spectrum, which has the contributions from successful and failed SNe. The average SN neutrino spectrum is in terms of average neutrino energy ($\langle E_\nu \rangle$), fraction of failed SNe (f_{BH}) and core-collapse supernova rate ($R_{\text{SN}}(0)$). However, these parameters are uncertain. Hence, we take a reference set ($\langle E_\nu \rangle = 15 \text{ MeV}$, $f_{\text{BH}} = 0.27$ and $R_{\text{SN}}(0) = 1 \times 10^{-4} \text{ yr}^{-1} \text{ Mpc}^{-3}$) and scan of a broad parameter region for sensitivity study.

3. Background prediction

The background sources are from the near reactor $\bar{\nu}_e$'s, fast neutron, cosmogenic ${}^9\text{Li}/{}^8\text{He}$ and atmospheric neutrino NC/charge current (CC) interactions, for which the NC interaction of atmospheric neutrinos with ${}^{12}\text{C}$ is one of the most significant source of the backgrounds, approximately one order magnitude of the DSNB signal [1].

Fast neutron background is induced by untagged muons that most of them only pass through the surrounding rock. The water as the protective aquifer is used to shield the fast neutrons, leading that most of fast neutrons capture in the top and equator region of the LS. Hence the spatial distribution of simulated fast neutron background dominates the fiducial volume. Via the balance of fast neutron background rate and target mass, a fiducial volume within Z and r_{XY} cut < 16 m is used in DSNB analysis. Due to total reflection ($R \equiv \sqrt{X^2 + Y^2 + Z^2} > 16$ m) and external radioactivity, there are two FV regions, one is FV1 ($R < 16$ m) and the other is FV2 ($R > 16$ m and Z and $r_{XY} < 16$ m), in which target mass is 14.7 kt and 3.6 kt, respectively.

The NC interactions of atmospheric neutrinos with ${}^{12}\text{C}$, where the emission of one neutron together with a prompt energy deposit, may be able to mimic the IBD coincidence signal of DSNB. We have performed a systematic study of the NC background induced by atmospheric neutrinos [4], which can be applied in the large LS detectors, such as JUNO for the DSNB study. The left panel of Fig. 1 illustrates the event rates and spectra of atmospheric NC backgrounds for the representative models. In the visible prompt energy window [12, 30] MeV, we obtain the total event rate of the IBD-like signals of the atmospheric NC interactions, as shown in the right panel of Fig. 1. Moreover, in the energy window, the right panel of Fig. 1 summarizes the exclusive event rates for six representative models, which have been categorized by the final-state products. The average rate of NC background of six models is estimated to $(3.0 \pm 0.5) \text{ kt}^{-1} \text{ yr}^{-1}$ for energy window from 12 MeV to 30 MeV. Note that the associated uncertainty is about 20%, representing the model variations.

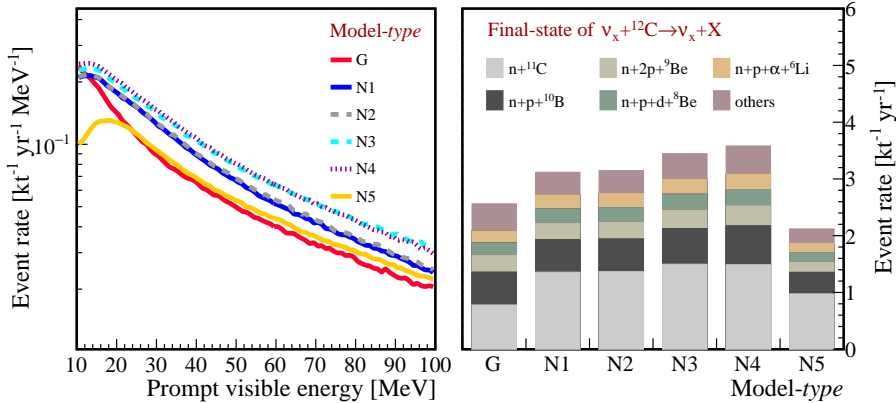


Figure 1: Event rates of the NC background as a function of the prompt energies (left panel). Event rates for the NC background within prompt energy window [12, 30] MeV in the exclusive channels (right panel).

Reducing the uncertainty of the NC background prediction is of prominent importance for the search for the DSNB at JUNO. The most crucial channel of the NC backgrounds is the ${}^{11}\text{C}$ channel

$(\nu_x + {}^{12}\text{C} \rightarrow \nu_x + n + {}^{11}\text{C})$, which has triple-coincident signals in LS, typically consisting of a prompt signal by fast-neutron recoil, a delayed signal by neutron capture on hydrogen and an additional signal from the unstable ${}^{11}\text{C}$ decaying at a later time. We develop a maximum-likelihood method to allow an *in situ* measurement of the NC interactions with a triple-coincidence signature after JUNO starts operation [5]. With JUNO data, we can evaluate the NC background uncertainty of the NC background for the DSNB search. Fig. 2 shows the relative uncertainty of NC background over JUNO running time (exposure), which is reproduced from the summary of Ref. [5]. The shaded bands represents the variations due to different scenarios on the LS radio purity and the rate of residual cosmogenic ${}^{11}\text{C}$. According to it, we can assume that for 1-3 years, 4-9 years, 10-20 years of JUNO running, the uncertainty of the background in DSNB sensitivity study is around 35%, 25% and 15%, respectively.

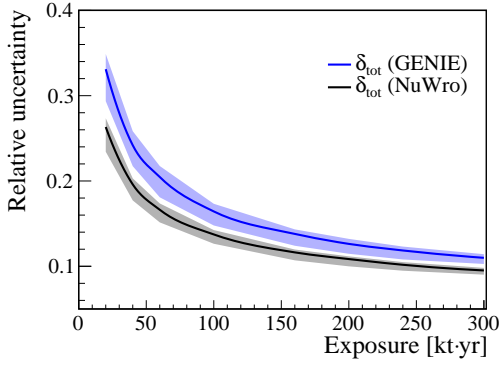


Figure 2: Relative uncertainty of NC background as a function of exposure.

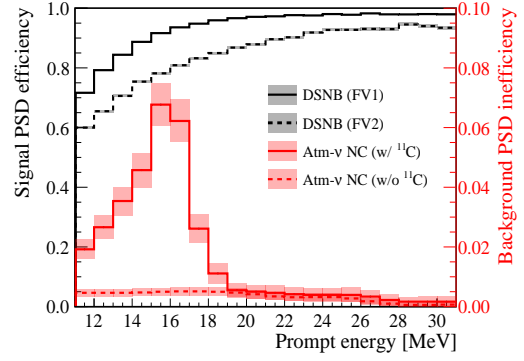


Figure 3: PSD efficiency in terms of prompt energy.

4. Background suppression

The typical predicted rate of DSNB signals in JUNO is about one order of magnitude smaller than the atmospheric NC background. However, the intrinsic pulse shape discrimination (PSD) capabilities of LS can suppress the NC background to an acceptable level, which is necessary to ultimately achieve an unambiguous discovery of the DSNB signal. Multivariate data analysis with ROOT (TMVA) [6] is applied for the PSD study. The characteristics from raw time profiles are extracted as variables, including the peak, tail shapes and the position-dependency. If the average residual NC background level is around 1% in the prompt energy window [12, 30] MeV, the DSNB signal efficiency is about 91% and 80% for FV1 and FV2, respectively. Given that the PSD performance is energy-dependent, it is necessary to estimate the PSD efficiency as a function of energy, which is taken for the sensitivity study. Hence, if the average inefficiency for NC background is about 1% in the prompt energy window [12, 30] MeV, the energy-dependent PSD efficiency is shown in Fig. 3, in which the shade bands represent the statistical uncertainty.

For the PSD study, the associated uncertainty is evaluated via the data samples similar to the atmospheric NC background and the DSNB signal from the future JUNO experimental data. From the MC study, we have obtained the statistics of such samples for different detector operation

periods, i.e., 1 year, 3 year, 9 year. Based on the PSD 1% inefficiency, the statistical uncertainty of these residual samples are about 40%, 20%, 10%, respectively. Therefore, the statistical uncertainty dominates in the study, and we evaluate the PSD uncertainty based on this uncertainty for different operation time.

5. Sensitivity

Fig. 4 summarizes the energy spectra of the DSNB signal and background before and after event selection, which includes the muon veto and energy-dependent PSD cut for FV1 and FV2 and triple-coincidence (TC) cut for the NC background associated with ^{11}C for FV1 only because of the quite high level of accidental background in FV2. It should be noted that the TC cut is independent of the prompt spectra but relied on the decay information of ^{11}C . The observation window for the prompt events is between 12 MeV to 30 MeV. One can note that after the event selection, the DSNB signal becomes visible in the observation window. The ratio of signal to background (S/B) is about 4.76 and 2.04 for FV1 and FV2, respectively, improving two order magnitude with the event selection.

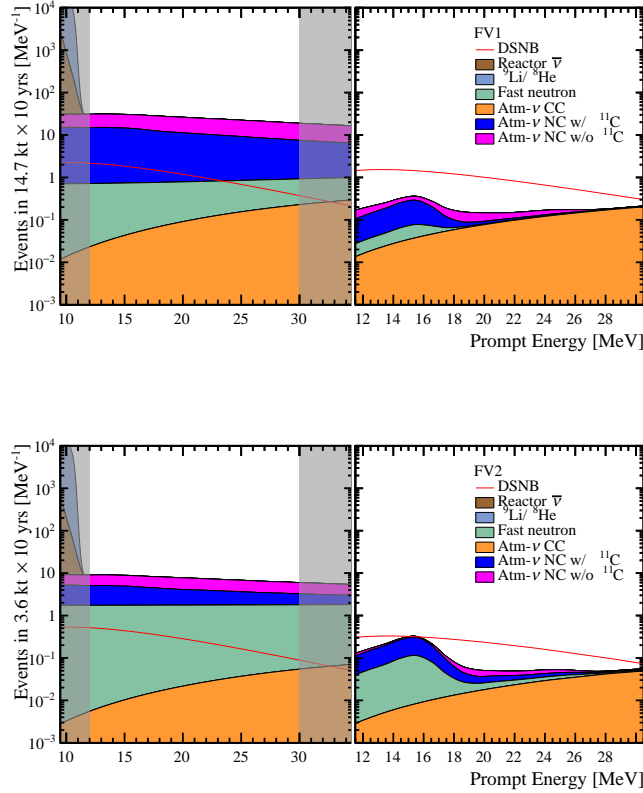


Figure 4: DSNB signal($R_{\text{SN}}(0) = 1.0 \times 10^{-4} \text{ yr}^{-1} \text{ Mpc}^{-3}$, $\langle E \rangle = 15 \text{ MeV}$, $f_{\text{BH}} = 0.27$) and background spectrum in FV1(top) and FV2(bottom) in JUNO (left)without and (right)with event selection.

In order to calculate the DSNB sensitivity, we employ the Possion-type log likelihood ratio (denoted as χ^2) as our test statistics, which is an energy-dependent fit of signal and background

spectra. The Asimov data set is used to define the medium sensitivity. In our case, the DSNB discovery sensitivity is defined as the difference between the minimal values of χ^2 with and without the DSNB signal after marginalization of other nuisance parameters and physical parameters.

In Fig. 5, we show the preliminary DSNB discovery potential as a function of the running time (within the fiducial volumes FV1 and FV2). For the nominal model, $\langle E_\nu \rangle$ is chosen as 15MeV, $R_{\text{CCSN}} = 1.0 \times 10^{-4} \text{yr}^{-1} \text{Mpc}^{-3}$ and $f_{\text{BH}} = 0.27$, represented by black solid line and black circle point in first panel and last two panels, respectively. For 1-3 years, 4-9 years and 10-20 years of running, the uncertainty of the background is assumed as 50%, 30% and 20%, respectively, which are the quadratic summation of uncertainties from the NC background calculation and the PSD efficiency. From the plots, one can see that, for the nominal model, the DSNB discovery potential can be achieved 3σ after 3 years data taking assuming 50% background uncertainty.

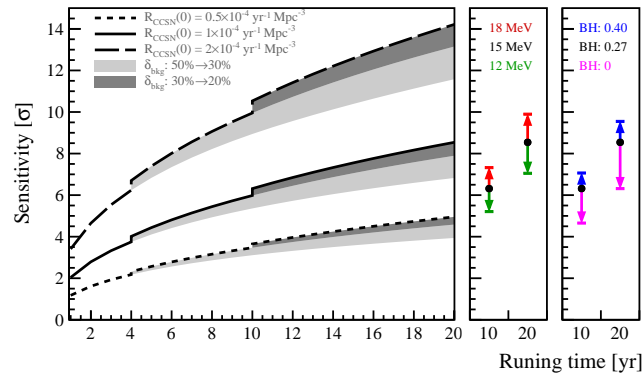


Figure 5: Sensitivity of DSNB as a function of the running time (within the fiducial volume 18.3 kt).

6. Summary

JUNO has great potential to detect the DSNB signal with its 20 kt LS and we have performed a systematic study of the detection of the DSNB with JUNO. The dominant background is from the NC interaction of atmospheric neutrinos with ^{12}C , which surpasses the DSNB by more than one order of magnitude. The NC background is precisely predicted from the spread of variety of data-driven models. A novel method of *in situ* measurement with 10 years of JUNO data can constrain the NC background rate within 15%. Besides, the PSD of LS as a powerful tool is developed to suppresses the atmospheric NC background and fast neutron background to be an acceptable level. The DSNB discovery potential can be achieved 3σ after 3 years data taking assuming the reference model of DSNB and 50% background uncertainty.

References

- [1] F. An *et al.* [JUNO Collaboration], *Neutrino Physics with JUNO*, *J. Phys. G* **43**, 030401 (2016).
- [2] A. Abusleme *et al.* [JUNO], *JUNO Physics and Detector*, [arXiv:2104.02565](https://arxiv.org/abs/2104.02565) [hep-ex].

- [3] A. Strumia and F. Vissani, *Precise quasielastic neutrino/nucleon cross-section*, *Phys. Lett. B* **564**, 42-54 (2003).
- [4] J. Cheng, Y. F. Li, L. J. Wen and S. Zhou, *Neutral-current background induced by atmospheric neutrinos at large liquid-scintillator detectors: I. model predictions*, *Phys. Rev. D* **103**, no.5, 053001 (2021).
- [5] J. Cheng, Y. F. Li, H. Q. Lu and L. J. Wen, *Neutral-current background induced by atmospheric neutrinos at large liquid-scintillator detectors. II. Methodology for insitu measurements*, *Phys. Rev. D* **103**, no.5, 053002 (2021).
- [6] A. Hocker, P. Speckmayer, J. Stelzer, J. Therhaag, E. von Toerne, H. Voss, M. Backes, T. Carli, O. Cohen and A. Christov, *et al. TMVA - Toolkit for Multivariate Data Analysis*, [arXiv:physics/0703039](https://arxiv.org/abs/physics/0703039) [physics.data-an].

Full Authors List: JUNO Collaboration

Angel Abusleme⁵, Thomas Adam⁴⁵, Shakeel Ahmad⁶⁶, Rizwan Ahmed⁶⁶, Sebastiano Aiello⁵⁵, Muhammad Akram⁶⁶, Feng-peng An²⁹, Qi An²², Giuseppe Andronico⁵⁵, Nikolay Anfimov⁶⁷, Vito Antonelli⁵⁷, Tatiana Antoshkina⁶⁷, Burin Asavapibhop⁷¹, João Pedro Athayde Marcondes de André⁴⁵, Didier Auguste⁴³, Andrej Babic⁷⁰, Nikita Balashov⁶⁷, Wander Baldini⁵⁶, Andrea Barresi⁵⁸, Davide Basilico⁵⁷, Eric Baussan⁴⁵, Marco Bellato⁶⁰, Antonio Bergnoli⁶⁰, Thilo Birkenfeld⁴⁸, Sylvie Blin⁴³, David Blum⁵⁴, Simon Blyth⁴⁰, Anastasia Bolshakova⁶⁷, Mathieu Bongrand⁴⁷, Clément Bordereau^{44,40}, Dominique Breton⁴³, Augusto Brigatti⁵⁷, Riccardo Brugnera⁶¹, Riccardo Bruno⁵⁵, Antonio Budano⁶⁴, Mario Buscemi⁵⁵, Jose Busto⁴⁶, Ilya Butorov⁶⁷, Anatael Cabrera⁴³, Hao Cai³⁴, Xiao Cai¹⁰, Yanke Cai¹⁰, Zhiyan Cai¹⁰, Riccardo Callegari⁶¹, Antonio Cammi⁵⁹, Agustin Campeny⁵, Chuanya Cao¹⁰, Guofu Cao¹⁰, Jun Cao¹⁰, Rossella Caruso⁵⁵, Cédric Cerna⁴⁴, Jinfan Chang¹⁰, Yun Chang³⁹, Pingping Chen¹⁸, Po-An Chen⁴⁰, Shaomin Chen¹³, Xurong Chen²⁶, Yi-Wen Chen³⁸, Yixue Chen¹¹, Yu Chen²⁰, Zhang Chen¹⁰, Jie Cheng¹⁰, Yaping Cheng⁷, Alexey Chetverikov⁶⁷, Davide Chiesa⁵⁸, Pietro Chimenti³, Artem Chukanov⁶⁷, Gérard Claverie⁴⁴, Catia Clementi⁶², Barbara Clerbaux², Selma Conforti Di Lorenzo⁴⁴, Daniele Corti⁶⁰, Flavio Dal Corso⁶⁰, Olivia Dalager⁷⁴, Christophe De La Taille⁴⁴, Jiawei Deng³⁴, Zhi Deng¹³, Ziyang Deng¹⁰, Wilfried Depnering⁵², Marco Diaz⁵, Xuefeng Ding⁵⁷, Yayun Ding¹⁰, Bayu Dirgantara⁷³, Sergey Dmitrievsky⁶⁷, Tadeas Dohnal⁴¹, Dmitry Dolzhikov⁶⁷, Georgy Donchenko⁶⁹, Jianmeng Dong¹³, Evgeny Doroshkevich⁶⁸, Marcos Dracos⁴⁵, Frédéric Druillolle⁴⁴, Ran Du¹⁰, Shuxian Du³⁷, Stefano Dusini⁶⁰, Martin Dvorak⁴¹, Timo Enqvist⁴², Heike Enzmann⁵², Andrea Fabbri⁶⁴, Lukas Faj⁷⁰, Donghua Fan²⁴, Lei Fan¹⁰, Jian Fang¹⁰, Wenxing Fang¹⁰, Marco Fargetta⁵⁵, Dmitry Fedoseev⁶⁷, Vladko Fekete⁷⁰, Li-Cheng Feng³⁸, Qichun Feng²¹, Richard Ford⁵⁷, Amélie Fournier⁴⁴, Haonan Gan³², Feng Gao⁴⁸, Alberto Garfagnini⁶¹, Arsenii Gavrikov⁶¹, Marco Giammarchi⁵⁷, Agnese Giaz⁶¹, Nunzio Giudice⁵⁵, Maxim Gonchar⁶⁷, Guanghua Gong¹³, Hui Gong¹³, Yuri Gornushkin⁶⁷, Alexandre Göttel^{50,48}, Marco Grassi⁶¹, Christian Grewing⁶⁷, Vasily Gromov⁶⁷, Minghao Gu¹⁰, Xiaofei Gu³⁷, Yu Gu¹⁹, Mengyun Guan¹⁰, Nunzio Guardone⁵⁵, Maria Gul⁶⁶, Cong Guo¹⁰, Jingyuan Guo²⁰, Wanlei Guo¹⁰, Xinheng Guo⁸, Yuhang Guo^{35,50}, Paul Hackspacher⁵², Caren Hagner⁴⁹, Ran Han⁷, Yang Han²⁰, Muhammad Sohaib Hassan⁶⁶, Miao He¹⁰, Wei He¹⁰, Tobias Heinz⁵⁴, Patrick Hellmuth⁴⁴, Yuekun Heng¹⁰, Rafael Herrera⁵, YuenKeung Hor²⁰, Shaojing Hou¹⁰, Yee Hsiung⁴⁰, Bei-Zhen Hu⁴⁰, Hang Hu²⁰, Jianrun Hu¹⁰, Jun Hu¹⁰, Shouyang Hu⁹, Tao Hu¹⁰, Zhuojun Hu²⁰, Chunhao Huang²⁰, Guihong Huang¹⁰, Hanxiong Huang⁹, Wenhao Huang²⁵, Xin Huang¹⁰, Xingtao Huang²⁵, Yongbo Huang²⁸, Jiaqi Hui³⁰, Lei Huo²¹, Wenju Huo²², Cédric Huss⁴⁴, Safeer Hussain⁶⁶, Ara Ioannisian¹, Roberto Isocrate⁶⁰, Beatrice Jelmini⁶¹, Kuo-Lun Jen³⁸, Ignacio Jeria⁵, Xiaolu Ji¹⁰, Xingzhao Ji²⁰, Huihui Jia³³, Junji Jia³⁴, Siyu Jian⁹, Di Jiang²², Wei Jiang¹⁰, Xiaoshan Jiang¹⁰, Ruyi Jin¹⁰, Xiaoping Jing¹⁰, Cécile Jollet⁴⁴, Jari Joutsenvaara⁴², Sirichok Jungthawan⁷³, Leonidas Kalousis⁴⁵, Philipp Kampmann⁵⁰, Li Kang¹⁸, Rebin Karaparambil⁴⁷, Narine Kazarian¹, Khanchai Khosonthongkee⁷³, Denis Korablev⁶⁷, Konstantin Kouzakov⁶⁹, Alexey Krasnoperov⁶⁷, Andre Kruth⁵¹, Nikolay Kutovskiy⁶⁷, Pasi Kuusiniemi⁴², Tobias Lachenmaier⁵⁴, Cecilia Landini⁵⁷, Sébastien Leblanc⁴⁴, Victor Lebrin⁴⁷, Frederic Lefevre⁴⁷, Ruiting Lei¹⁸, Rupert Leitner⁴¹, Jason Leung³⁸, Demin Li³⁷, Fei Li¹⁰, Fule Li¹³, Haitao Li²⁰, Huiling Li¹⁰, Jiaqi Li²⁰, Mengzhao Li¹⁰, Min Li¹¹, Nan Li¹⁰, Nan Li¹⁶, Qingjiang Li¹⁶, Ruhui Li¹⁰, Shanfang Li¹⁸, Tao Li²⁰, Weidong Li^{10,14}, Weiguo Li¹⁰, Xiaomei Li⁹, Xiaonan Li¹⁰, Xinglong Li⁹, Yi Li¹⁸, Yufeng Li¹⁰, Zhaohan Li¹⁰, Zhibing Li²⁰, Ziyuan Li²⁰, Hao Liang⁹, Hao Liang²², Jiajun Liao²⁰, Daniel Liebau⁵¹, Ayut Limphirat⁷³, Sukit Limpjummong⁷³, Guey-Lin Lin³⁸, Shengxin Lin¹⁸, Tao Lin¹⁰, Jiajie Ling²⁰, Ivano Lippi⁶⁰, Fang Liu¹¹, Haidong Liu³⁷, Hongbang Liu²⁸, Hongjuan Liu²³, Hongtao Liu²⁰, Hui Liu¹⁹, Jianglai Liu^{30,31}, Jinchang Liu¹⁰, Min Liu²³, Qian Liu¹⁴, Qin Liu²², Runxuan Liu^{50,48}, Shuangyu Liu¹⁰, Shubin Liu²², Shulin Liu¹⁰, Xiaowei Liu²⁰, Xiwen Liu²⁸, Yan Liu¹⁰, Yunzhe Liu¹⁰, Alexey Lokhov^{69,68}, Paolo Lombardi⁵⁷, Claudio Lombardo⁵⁵, Kai Loo⁵², Chuan Lu³², Haoqi Lu¹⁰, Jingbin Lu¹⁵, Jinguang Lu¹⁰, Shuxiang Lu³⁷, Xiaoxu Lu¹⁰, Bayarto Lubsandorzhev⁶⁸, Sultim Lubsandorzhev⁶⁸, Livia Ludhova^{50,48}, Arslan Lukanov⁶⁸, Fengjiao Luo¹⁰, Guang Luo²⁰, Pengwei Luo²⁰, Shu Luo³⁶, Wuming Luo¹⁰, Vladimir Lyashuk⁶⁸, Bangzheng Ma²⁵, Qiumei Ma¹⁰, Si Ma¹⁰, Xiaoyan Ma¹⁰, Xubo Ma¹¹, Jihane Maalmi⁴³, Yury Malyskin⁶⁷, Roberto Carlos Mandujano⁶⁷, Fabio Mantovani⁵⁶, Francesco Manzali⁶¹, Xin Mao⁷, Yajun Mao¹², Stefano M. Mari⁶⁴, Filippo Marini⁶¹, Sadia Marium⁶⁶, Cristina Martellini⁶⁴, Gisele Martin-Chassard⁴³, Agnese Martini⁶³, Matthias Mayer⁵³, Davit Mayilyan¹, Ints Mednieks⁶⁵, Yue Meng³⁰, Anselmo Meregalia⁴⁴, Emanuela Meroni⁵⁷, David Meyhöfer⁴⁹, Mauro Mezzetto⁶⁰, Jonathan Miller⁶, Lino Miramonti⁵⁷, Paolo Montini⁶⁴, Michele Montuschi⁵⁶, Axel Müller⁵⁴, Massimiliano Nastasi⁵⁸, Dmitry V. Naumov⁶⁷, Elena Naumova⁶⁷, Diana Navas-Nicolas⁴³, Igor Nemchenok⁶⁷, Minh Thuan Nguyen Thi³⁸, Feipeng Ning¹⁰, Zhe Ning¹⁰, Hiroshi Nunokawa⁴, Lothar Oberauer⁵³, Juan Pedro Ochoa-Ricoux^{74,5}, Alexander Olshevskiy⁶⁷, Domizia Orestano⁶⁴, Fausto Ortica⁶², Rainer Othegraven⁵², Hsiao-Ru Pan⁴⁰, Alessandro Paoloni⁶³, Sergio Parmeggiano⁵⁷, Yatian Pei¹⁰, Nicomede Pelliccia⁶², Anguo Peng²³, Haiping Peng²², Frédéric Perrot⁴⁴, Pierre-Alexandre Petitjean², Fabrizio Petrucci⁶⁴, Oliver Pilarczyk⁵², Luis Felipe Piñeres Rico⁴⁵, Artyom Popov⁶⁹, Pascal Poussot⁴⁵, Wathan Pratumwan⁷³, Ezio Previtali⁵⁸, Fazhi Qi¹⁰, Ming Qi²⁷, Sen Qian¹⁰, Xiaohui Qian¹⁰, Zhen Qian²⁰, Hao Qiao¹², Zhonghua Qin¹⁰, Shoukang Qiu²³, Muhammad Usman Rajput⁶⁶, Gioacchino Ranucci⁵⁷, Neill Raper²⁰, Alessandria Re⁵⁷, Henning Reber⁴⁹, Abdel Rebi⁴⁴, Bin Ren¹⁸, Jie Ren⁹, Barbara Ricci⁵⁶, Markus Robens⁵¹, Mathieu Roche⁴⁴, Narongkiat Rodphai⁷¹, Aldo Romani⁶², Bedřich Roskovec⁴¹, Christian Roth⁵¹, Xiangdong Ruan²⁸, Xichao Ruan⁹, Saroj Rujirawat⁷³, Arseniy Rybnikov⁶⁷, Andrey Sadovsky⁶⁷, Paolo Saggese⁵⁷, Simone Sanfilippo⁶⁴, Anut Sangka⁷², Nuanwan Sanguansak⁷³, Utane Sawangwit⁷², Julia Sawatzki⁵³, Fatma Sawy⁶¹, Michaela Schever^{50,48}, Cédric Schwab⁴⁵, Konstantin Schweizer⁵³, Alexandr Selyunin⁶⁷, Andrea Serafini⁵⁶, Giulio Settanta⁵⁰, Mariangela Settimo⁴⁷, Zhuang Shao³⁵, Vladislav Sharov⁶⁷, Arina Shaydurova⁶⁷, Jingyan Shi¹⁰, Yanan Shi¹⁰, Vitaly Shutov⁶⁷, Andrey Sidorenkov⁶⁸, Fedor Simkovic⁷⁰, Chiara Sirignano⁶¹, Jaruchit Siripak⁷³, Monica Sisti⁵⁸, Maciej Słupecki⁴², Mikhail Smirnov²⁰, Oleg Smirnov⁶⁷, Thiago Sogo-Bezerra⁴⁷, Sergey Sokolov⁶⁷, Julianan Songwadhana⁷³, Boonrucksar Soonthornthum⁷², Albert Sotnikov⁶⁷, Ondřej Šrámek⁴¹, Warintorn Sreethawong⁷³, Achim Stahl⁴⁸, Luca Stanco⁶⁰, Konstantin Stankevich⁶⁹, Dušan Štefánik⁷⁰, Hans Steiger^{52,53}, Jochen Steinmann⁴⁸, Tobias Sterr⁵⁴, Matthias Raphael Stock⁵³, Virginia Strati⁵⁶, Alexander Studenikin⁶⁹, Shifeng Sun¹¹, Xilei Sun¹⁰, Yongjie Sun²², Yongzhao Sun¹⁰, Narumon Suwonjandee⁷¹, Michal Szelezniak⁴⁵, Jian Tang²⁰, Qiang Tang²⁰, Quan Tang²³, Xiao Tang¹⁰, Alexander Tietzsch⁵⁴, Igor Tkachev⁶⁸, Tomas Tmej⁴¹, Marco Danilo Claudio Torri⁴¹, Konstantin Treskov⁶⁷, Andrea Triossi⁴⁵, Giancarlo Troni⁵, Wladyslaw Trzaska⁴², Cristina Tuve⁵⁵, Nikita Ushakov⁶⁸, Johannes

van den Boom⁵¹, Stefan van Waasen⁵¹, Guillaume Vanroyen⁴⁷, Vadim Vedin⁶⁵, Giuseppe Verde⁵⁵, Maxim Vialkov⁶⁹, Benoit Viaud⁴⁷, Moritz Vollbrecht^{50,48}, Cristina Volpe⁴³, Vit Vorobel⁴¹, Dmitriy Voronin⁶⁸, Lucia Votano⁶³, Pablo Walker⁵, Caishen Wang¹⁸, Chung-Hsiang Wang³⁹, En Wang³⁷, Guoli Wang²¹, Jian Wang²², Jun Wang²⁰, Kunyu Wang¹⁰, Lu Wang¹⁰, Meifen Wang¹⁰, Meng Wang²³, Meng Wang²⁵, Ruiguang Wang¹⁰, Siguang Wang¹², Wei Wang²⁷, Wei Wang²⁰, Wenshuai Wang¹⁰, Xi Wang¹⁶, Xiangyu Wang²⁰, Yangfu Wang¹⁰, Yaoguang Wang¹⁰, Yi Wang¹³, Yi Wang²⁴, Yifang Wang¹⁰, Yuanqing Wang¹³, Yuman Wang²⁷, Zhe Wang¹³, Zheng Wang¹⁰, Zhimin Wang¹⁰, Zongyi Wang¹³, Muhammad Waqas⁶⁶, Apimook Watcharakool⁷², Lianghong Wei¹⁰, Wei Wei¹⁰, Wenlu Wei¹⁰, Yadong Wei¹⁸, Kaile Wen¹⁰, Liangjian Wen¹⁰, Christopher Wiebusch⁴⁸, Steven Chan-Fai Wong²⁰, Bjoern Wonsak⁴⁹, Diru Wu¹⁰, Qun Wu²⁵, Zhi Wu¹⁰, Michael Wurm⁵², Jacques Wurtz⁴⁵, Christian Wysotzki⁴⁸, Yufei Xi³², Dongmei Xia¹⁷, Xiaochuan Xie¹⁷, Yuguang Xie¹⁰, Zhangquan Xie¹⁰, Zhizhong Xing¹⁰, Benda Xu¹³, Cheng Xu²³, Donglian Xu^{31,30}, Fanrong Xu¹⁹, Hangkun Xu¹⁰, Jilei Xu¹⁰, Jing Xu⁸, Meihang Xu¹⁰, Yin Xu³³, Yu Xu^{50,48}, Baojun Yan¹⁰, Taylor Yan⁷³, Wenqi Yan¹⁰, Xiongbo Yan¹⁰, Yupeng Yan⁷³, Anbo Yang¹⁰, Changgen Yang¹⁰, Chengfeng Yang²⁸, Huan Yang¹⁰, Jie Yang³⁷, Lei Yang¹⁸, Xiaoyu Yang¹⁰, Yifan Yang¹⁰, Yifan Yang², Haifeng Yao¹⁰, Zafar Yasin⁶⁶, Jiakuan Ye¹⁰, Mei Ye¹⁰, Ziping Ye³¹, Ugur Yegin⁵¹, Frédéric Yermia⁴⁷, Peihuai Yi¹⁰, Na Yin²⁵, Xiangwei Yin¹⁰, Zhengyun You²⁰, Boxiang Yu¹⁰, Chiye Yu¹⁸, Chunxu Yu³³, Hongzhao Yu²⁰, Miao Yu³⁴, Xianghui Yu³³, Zeyuan Yu¹⁰, Zezhong Yu¹⁰, Chengzhuo Yuan¹⁰, Ying Yuan¹², Zhenxiong Yuan¹³, Ziyi Yuan³⁴, Baobiao Yue²⁰, Noman Zafar⁶⁶, Andre Zambanini⁵¹, Vitalii Zavadskyi⁶⁷, Shan Zeng¹⁰, Tingxuan Zeng¹⁰, Yuda Zeng²⁰, Liang Zhan¹⁰, Aiqiang Zhang¹³, Feiyang Zhang³⁰, Guoqing Zhang¹⁰, Haiqiong Zhang¹⁰, Honghao Zhang²⁰, Jiawen Zhang¹⁰, Jie Zhang¹⁰, Jin Zhang²⁸, Jingbo Zhang²¹, Jinnan Zhang¹⁰, Peng Zhang¹⁰, Qingmin Zhang³⁵, Shiqi Zhang²⁰, Shu Zhang²⁰, Tao Zhang³⁰, Xiaomei Zhang¹⁰, Xuantong Zhang¹⁰, Xueyao Zhang²⁵, Yan Zhang¹⁰, Yinhong Zhang¹⁰, Yiyu Zhang¹⁰, Yongpeng Zhang¹⁰, Yuanyuan Zhang³⁰, Yumei Zhang²⁰, Zhenyu Zhang³⁴, Zhijian Zhang¹⁸, Fengyi Zhao²⁶, Jie Zhao¹⁰, Rong Zhao²⁰, Shujun Zhao³⁷, Tianchi Zhao¹⁰, Dongqin Zheng¹⁹, Hua Zheng¹⁸, Minshan Zheng⁹, Yangheng Zheng¹⁴, Weirong Zhong¹⁹, Jing Zhou⁹, Li Zhou¹⁰, Nan Zhou²², Shun Zhou¹⁰, Tong Zhou¹⁰, Xiang Zhou³⁴, Jiang Zhu²⁰, Kangfu Zhu³⁵, Kejun Zhu¹⁰, Zhihang Zhu¹⁰, Bo Zhuang¹⁰, Honglin Zhuang¹⁰, Liang Zong¹³ and Jiaheng Zou¹⁰ ¹Yerevan Physics Institute, Yerevan, Armenia.

²Université Libre de Bruxelles, Brussels, Belgium.

³Universidade Estadual de Londrina, Londrina, Brazil.

⁴Pontificia Universidade Católica do Rio de Janeiro, Rio, Brazil.

⁵Pontificia Universidad Católica de Chile, Santiago, Chile.

⁶Universidad Tecnica Federico Santa Maria, Valparaiso, Chile.

⁷Beijing Institute of Spacecraft Environment Engineering, Beijing, China.

⁸Beijing Normal University, Beijing, China.

⁹China Institute of Atomic Energy, Beijing, China.

¹⁰Institute of High Energy Physics, Beijing, China.

¹¹North China Electric Power University, Beijing, China.

¹²School of Physics, Peking University, Beijing, China.

¹³Tsinghua University, Beijing, China.

¹⁴University of Chinese Academy of Sciences, Beijing, China.

¹⁵Jilin University, Changchun, China.

¹⁶College of Electronic Science and Engineering, National University of Defense Technology, Changsha, China.

¹⁷Chongqing University, Chongqing, China.

¹⁸Dongguan University of Technology, Dongguan, China.

¹⁹Jinan University, Guangzhou, China.

²⁰Sun Yat-Sen University, Guangzhou, China.

²¹Harbin Institute of Technology, Harbin, China.

²²University of Science and Technology of China, Hefei, China.

²³The Radiochemistry and Nuclear Chemistry Group in University of South China, Hengyang, China.

²⁴Wuyi University, Jiangmen, China.

²⁵Shandong University, Jinan, China, and Key Laboratory of Particle Physics and Particle Irradiation of Ministry of Education, Shandong University, Qingdao, China.

²⁶Institute of Modern Physics, Chinese Academy of Sciences, Lanzhou, China.

²⁷Nanjing University, Nanjing, China.

²⁸Guangxi University, Nanning, China.

²⁹East China University of Science and Technology, Shanghai, China.

³⁰School of Physics and Astronomy, Shanghai Jiao Tong University, Shanghai, China.

³¹Tsung-Dao Lee Institute, Shanghai Jiao Tong University, Shanghai, China.

³²Institute of Hydrogeology and Environmental Geology, Chinese Academy of Geological Sciences, Shijiazhuang, China.

³³Nankai University, Tianjin, China.

³⁴Wuhan University, Wuhan, China.

³⁵Xi'an Jiaotong University, Xi'an, China.

³⁶Xiamen University, Xiamen, China.

³⁷School of Physics and Microelectronics, Zhengzhou University, Zhengzhou, China.

³⁸Institute of Physics, National Yang Ming Chiao Tung University, Hsinchu.

³⁹National United University, Miao-Li.

- ⁴⁰Department of Physics, National Taiwan University, Taipei.
- ⁴¹Charles University, Faculty of Mathematics and Physics, Prague, Czech Republic.
- ⁴²University of Jyväskylä, Department of Physics, Jyväskylä, Finland.
- ⁴³IJCLab, Université Paris-Saclay, CNRS/IN2P3, 91405 Orsay, France.
- ⁴⁴Univ. Bordeaux, CNRS, CENBG, UMR 5797, F-33170 Gradignan, France.
- ⁴⁵IPHC, Université de Strasbourg, CNRS/IN2P3, F-67037 Strasbourg, France.
- ⁴⁶Centre de Physique des Particules de Marseille, Marseille, France.
- ⁴⁷SUBATECH, Université de Nantes, IMT Atlantique, CNRS-IN2P3, Nantes, France.
- ⁴⁸III. Physikalisches Institut B, RWTH Aachen University, Aachen, Germany.
- ⁴⁹Institute of Experimental Physics, University of Hamburg, Hamburg, Germany.
- ⁵⁰Forschungszentrum Jülich GmbH, Nuclear Physics Institute IKP-2, Jülich, Germany.
- ⁵¹Forschungszentrum Jülich GmbH, Central Institute of Engineering, Electronics and Analytics - Electronic Systems (ZEA-2), Jülich, Germany.
- ⁵²Institute of Physics, Johannes-Gutenberg Universität Mainz, Mainz, Germany.
- ⁵³Technische Universität München, München, Germany.
- ⁵⁴Eberhard Karls Universität Tübingen, Physikalisches Institut, Tübingen, Germany.
- ⁵⁵INFN Catania and Dipartimento di Fisica e Astronomia dell'Università di Catania, Catania, Italy.
- ⁵⁶Department of Physics and Earth Science, University of Ferrara and INFN Sezione di Ferrara, Ferrara, Italy.
- ⁵⁷INFN Sezione di Milano and Dipartimento di Fisica dell'Università di Milano, Milano, Italy.
- ⁵⁸INFN Milano Bicocca and University of Milano Bicocca, Milano, Italy.
- ⁵⁹INFN Milano Bicocca and Politecnico of Milano, Milano, Italy.
- ⁶⁰INFN Sezione di Padova, Padova, Italy.
- ⁶¹Dipartimento di Fisica e Astronomia dell'Università di Padova and INFN Sezione di Padova, Padova, Italy.
- ⁶²INFN Sezione di Perugia and Dipartimento di Chimica, Biologia e Biotecnologie dell'Università di Perugia, Perugia, Italy.
- ⁶³Laboratori Nazionali di Frascati dell'INFN, Roma, Italy.
- ⁶⁴University of Roma Tre and INFN Sezione Roma Tre, Roma, Italy.
- ⁶⁵Institute of Electronics and Computer Science, Riga, Latvia.
- ⁶⁶Pakistan Institute of Nuclear Science and Technology, Islamabad, Pakistan.
- ⁶⁷Joint Institute for Nuclear Research, Dubna, Russia.
- ⁶⁸Institute for Nuclear Research of the Russian Academy of Sciences, Moscow, Russia.
- ⁶⁹Lomonosov Moscow State University, Moscow, Russia.
- ⁷⁰Comenius University Bratislava, Faculty of Mathematics, Physics and Informatics, Bratislava, Slovakia.
- ⁷¹Department of Physics, Faculty of Science, Chulalongkorn University, Bangkok, Thailand.
- ⁷²National Astronomical Research Institute of Thailand, Chiang Mai, Thailand.
- ⁷³Suranaree University of Technology, Nakhon Ratchasima, Thailand.
- ⁷⁴Department of Physics and Astronomy, University of California, Irvine, California, USA.